

9th International Conference Interdisciplinarity in Engineering, INTER-ENG 2015, 8-9 October 2015, Tirgu-Mures, Romania

## Simulating the Effect of Gas Channel Geometry on PEM Fuel Cell Performance by Finite Element Method

Viorel Ionescu<sup>a,\*</sup>

<sup>a</sup>*Department of Physics and Electronics, Ovidius University, Constanta, 900527, Romania*

---

### Abstract

Proton exchange membrane fuel cells (PEMFC) become in the last years an attractive alternative clean energy source and the main researches are oriented in order to understand how different cell parameters affects the performance of the fuel cell in real operating conditions and subsequently reduce the cost involved in prototype development. Comsol Multiphysics, a commercial solver based on the Finite Element Method (FEM) was used for developing a three dimensional model of PEMFC working at a high temperature of 150 °C. Cathode gas flow velocity influence on the cell performance was investigated at first. The effect of channel width and channel height on the current density at a cell voltage of 0.5 V was established, at various cathode gas flow velocities between 0.04 and 0.42 m/s. Local current density variation for cell geometries with three different channel widths (0.8, 1.2 and 1.6 mm) at three different channel heights (1, 2 and 3 mm) were computed at a cathode inlet flow velocity of 0.1 m/s and cell voltage of 0.3V. Oxygen and water molar concentrations at cathode catalyst layer-GDL channel interface were also studied for specific gas channel geometries.

© 2016 Published by Elsevier Ltd. This is an open access article under the CC BY-NC-ND license

(<http://creativecommons.org/licenses/by-nc-nd/4.0/>).

Peer-review under responsibility of the “Petru Maior” University of Tirgu Mures, Faculty of Engineering

**Keywords:** Fuel cell; polarization curve; molar concentration; flow velocity; gas channel.

---

---

\* Corresponding author. Tel.: +40-766-653755

E-mail address: [v\\_ionescu@univ-ovidius.ro](mailto:v_ionescu@univ-ovidius.ro)

## 1. Introduction

PEM fuel cells are the most promising candidates as energy converters, especially for automobile applications, being used in a clean hybrid power supply system and providing the rated power to the load [1,2]. Nevertheless, the wide application of a PEMFC is limited due to high capital cost, fuel availability and durability and the difficulty of maintaining suitable thermal management and water management also affects the fuel cell performance significantly [3,4]. When the water removal rate exceeds the water generation rate, membrane dehydration occurs, producing performance degradation due to significant ohmic losses within the cell [5].

There are research advances of high temperature PEM fuel cells (HT-PEMFCs) with polybenzimidazole (PBI) - based membrane in various fields because there are several reasons for operating at temperatures above  $100^{\circ}\text{C}$  [6]: enhancing of the electrochemical kinetics for the cell reactions, simplicity of the cooling system due to the increased temperature gradient between the fuel cell stack and the coolant, increasing of the CO tolerance which enables utilization of lower quality reformed hydrogen.

Various studies have devoted to developing mathematical bi-dimensional models for the transport of reactants and product water in a PEMFC. Berning and Djilali presented a 3-dimensional, multi-phase and multi-component model for anode and cathode of PEMFC [7]. They described the two phase flow inside the gas diffusion layer (GDL) by the unsaturated flow theory (UFT) that a uniform gas phase pressure is assumed within the GDL.

The 3D HT-PEMFC numerical model used in this paper is derived from 3D single-phase isothermal model developed by E.U. Ubong et al. [8] to predict the performance of a HT-PEMFC with a PBI membrane.

The objective of this work is to investigate the effect of cathode gas flow velocity and gas channel geometry (width and height) on the cell performance with the help of a 3D model using commercial FEM package Comsol Multiphysics (version 4.2).

## 2. Model set-up

The 3D computational domain includes a section of the PBI membrane and both cathode and anode gas flow channels, GDLs, and catalyst layers (see Fig. 1).

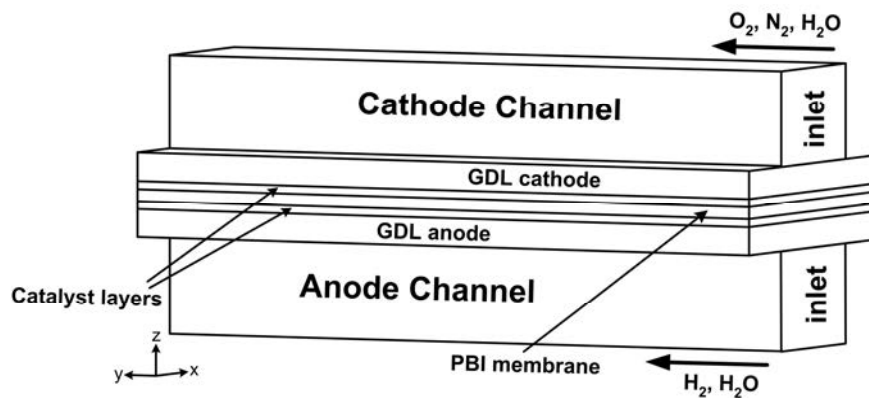


Fig. 1. 3D HT-PEMFC computational model geometry.

At steady state, single-phase, isothermal model of PEM fuel cell consists of five principles of conservation: mass, momentum, species, energy and charge. COMSOL Multiphysics are used to solve this complex HTPM fuel cell model. The conservation equations are solved sequentially (and grouped) for various variables, such as: velocity vector, pressure, mass/mole fraction of the species, electric and protonic phase potentials, solid and fluid – gas – phase temperatures. Momentum transfer is modeled using Free and Porous Media Flow interface.

The operating conditions and parameters of the base model are given in Table 1.

Table 1. Design and operating parameters

Parameter	Value
Reference pressure (Pa)	101325
Cell voltage (V)	0.9
Temperature(°C)	150
Oxygen reference concentration (mole/m <sup>3</sup> )	40.88
Hydrogen reference concentration (mole/m <sup>3</sup> )	40.88
Inlet H <sub>2</sub> mass fraction (anode)	0.743
Inlet H <sub>2</sub> O mass fraction (cathode)	0.18
Inlet O <sub>2</sub> mass fraction (cathode)	0.228
H <sub>2</sub> -H <sub>2</sub> O Binary diffusion coefficient (10 <sup>-4</sup> m <sup>2</sup> /s)	1.603
N <sub>2</sub> -H <sub>2</sub> O Binary diffusion coefficient (10 <sup>-5</sup> m <sup>2</sup> /s)	4.48
O <sub>2</sub> -N <sub>2</sub> binary diffusion coefficient (10 <sup>-5</sup> m <sup>2</sup> /s)	4.18
O <sub>2</sub> -H <sub>2</sub> O binary diffusion coefficient (10 <sup>-5</sup> m <sup>2</sup> /s)	4.91
Anode inlet flow velocity (m/s)	0.17
Cathode inlet flow velocity (m/s)	0.42
Anode viscosity (10 <sup>-5</sup> Pa·s)	1.12
Cathode viscosity (10 <sup>-5</sup> Pa·s)	2.68
Cell length (cm)	2
Gas channel width (mm)	0.4 – 2.4
Gas channel height (mm)	0.5 - 3
Width of the shoulder (mm)	0.9
Catalyst layer thickness (μm)	50
Catalyst layer permeability (m <sup>2</sup> )	2.36 × 10 <sup>-12</sup>
Catalyst layer porosity	0.2
Open volume fraction for gas diffusion in catalyst layer	0.4
PBI/H <sub>3</sub> PO <sub>4</sub> membrane thickness (μm)	98
PBI/H <sub>3</sub> PO <sub>4</sub> membrane conductivity (S/m)	1.74
GDL conductivity (S/m)	222
GDL bulk porosity	0.4
GDL permeability coefficient (× 10 <sup>-11</sup> m <sup>2</sup> )	1.8
GDL thickness (μm)	380

Laminar flow in the channels is described by the Navier-Stokes equations (dimensionless formulation), for the steady state in case of no external forces:

$$(\mathbf{v} \cdot \nabla) \mathbf{v} + \nabla p - \frac{1}{R_e} \nabla (\nabla \mathbf{v} + (\nabla \mathbf{v})^T) = 0; \quad \nabla \cdot \mathbf{v} = 0 \quad (1)$$

where unknown depended variables are  $p$  – pressure and  $\mathbf{v}$  – velocity;  $R_e$  is a dimensionless Reynolds number.

Porous gas diffusion layers (GDLs) and electrode flow can be given by a similar set of differential equations, when the Brinkman formulation is used:

$$k\mathbf{v} + \nabla p - \frac{1}{R_e} \nabla (\nabla \mathbf{v} + (\nabla \mathbf{v})^T) = 0$$

$$\nabla \cdot \mathbf{v} = 0 \quad (2)$$

where  $k$  is the Brinkman parameter, defined as:  $k = \frac{H^2}{R_e \cdot \kappa}$ , with  $H$  – channel height and  $\kappa$  - permeability.

Conservation of species was solved for the flow channels, GDLs and porous electrode using the Maxwell Stefan equations in two different Transport of Concentrated Species interfaces.

It solves for the fluxes of each species (H<sub>2</sub> and H<sub>2</sub>O in the anode compartment, O<sub>2</sub> and H<sub>2</sub>O in the cathode compartment) in terms of mass fraction. The Maxwell-Stefan equation, defined for each component from the mixture of the three gases, is presented below [9]:

$$\nabla \cdot [-\rho \omega_i \sum_{j=1}^3 D_{ij} \left\{ \frac{M}{M_j} \left( \nabla \omega_j + \omega_j \frac{\nabla M}{M} \right) + (x_j - \omega_j) \frac{\nabla p}{p} \right\} + \omega_i \rho v] = 0 \quad (3)$$

In Equation (3),  $x_j$  is the molar fraction of each gas  $j$ , parameters  $\omega_i$  and  $\omega_j$  are the mass fractions of gases  $i$  and  $j$  respectively, parameter  $\rho$  is the overall mass density of the air mixture obtained from the ideal gas law,  $D_{ij}$  is the binary diffusion coefficient,  $M$  is the total molar mass of the mixture and  $M_j$  is the molecular weight of gas  $j$ .

Conservation of the electric charge is based on two currents: an ionic current formed by the protons travelling through the membrane and an electronic current formed by the electrons passing through the solid matrix of electrodes. The current continuity equations are obtained by using Ohm's law [8]:

$$\begin{aligned} \nabla \cdot (-\sigma_s \nabla \cdot \phi_s) &= S_s \\ \nabla \cdot (-\sigma_m \nabla \cdot \phi_m) &= S_m \end{aligned} \quad (4)$$

where  $\Phi$  is the phase potential,  $\sigma$  is the effective electric conductivity (S/m),  $S$  is the current source term ( $A \cdot m^{-3}$ ) and subscripts  $s$  and  $m$  denotes the properties of the solid phase and membrane, respectively. At anode catalyst layer,  $S_m = j_a$  and  $S_s = -j_a$ ; at cathode catalyst layer,  $S_m = j_c$  and  $S_s = -j_c$ . Here,  $j_a$  and  $j_c$  are the transfer current density corresponding to the electrochemical reaction at the anode and cathode catalyst layers, respectively.

Transfer current densities were calculated by using a simplified Butler-Volmer equation [9].

### 3. Results and discussions

Fig. 2 showed the effect of changing the cathode gas flow velocity at values under 0.42 m/s on the fuel cell performance, for a cathode channel having width of 0.8 mm and height of 1 mm. When the gas flow velocity is increased from 0.02 to 0.12 m/s, the fuel cell performance is clearly enhanced, especially at lower operating fuel cell voltages.

The rate of the electrochemical reaction is increased due to the increase in oxygen gas through the gas diffusion layer to reaction sites. Due to the low membrane humidification, this enhancing performance effect is minimal at high operating voltages. So, the air stream is able to supply oxygen with the required rate for gas flow velocity values over 0.1 m/s on this cell model.

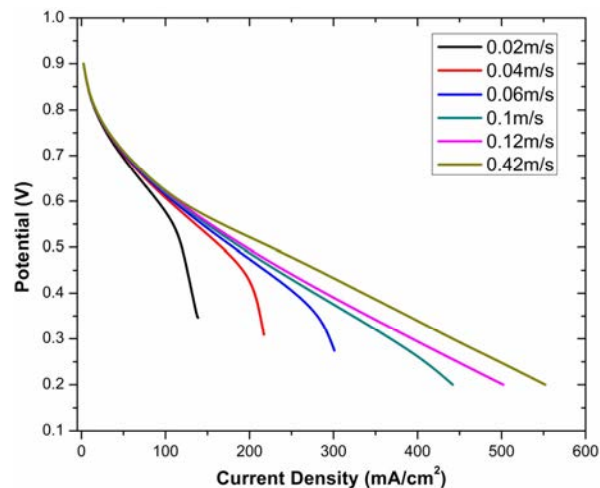


Fig. 2. Effect of cathode gas flow velocity on cell performance at base conditions for different cathode inlet flow velocities (between 0.02 and 0.42 m/s).

Fig.3 displayed the effect of channel width variation at a constant height of 1 mm and the effect of channel height variation at a constant width of 0.8 mm on the current density for different gas flow velocities.

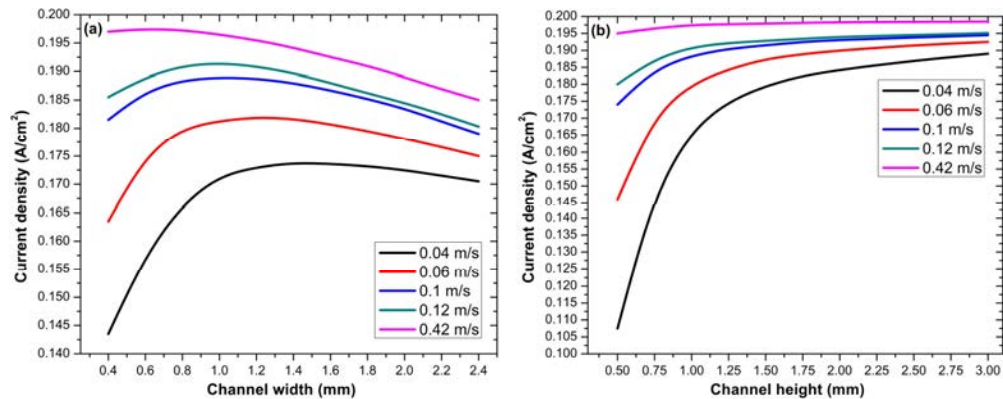


Fig. 3. Effect of channel width (a) and channel height (b) on PEM fuel cell current density at cell potential of 0.5V for various cathode gas flow velocities.

Fig. 3.a indicated that current density attained a maximum value at one specific value of gas flow velocity, different from a value to another value of this velocity. For example, at 0.04 m/s current density was maxim for a channel width of 1.6 mm and at 0.42 m/s current density was maxim for a channel width of 0.8 mm.

Fig. 3.b illustrated a rapid increase of current density from 0.5 to 0.75 mm for all cathode gas flow velocities investigated. No significant change in current density was registered starting with a value of 1 mm for the channel width at flow velocities higher than 0.1 m/s; between the values of 1.25 and 3 mm for the channel height, current density varies very slowly, rising with about 2.5 – 7% from the value registered at 1 mm.

From now on, all the simulations were performed at a cell voltage of 0.3 V and at a cathode gas flow velocity of 0.1 m/s.

Fig. 4 presented the local current density variation at the cathode catalyst layer – GDL channel interface along the cell height at channel widths of 0.8, 1.2 and 1 mm for different channel depths: 1, 2 and 3 mm.

It can be seen from this figure that the current generation is more non-uniform in the case of 1 mm depth channel for all the geometries investigated. At higher channel depths, more amount of air and hence oxygen enter the cathode channel.

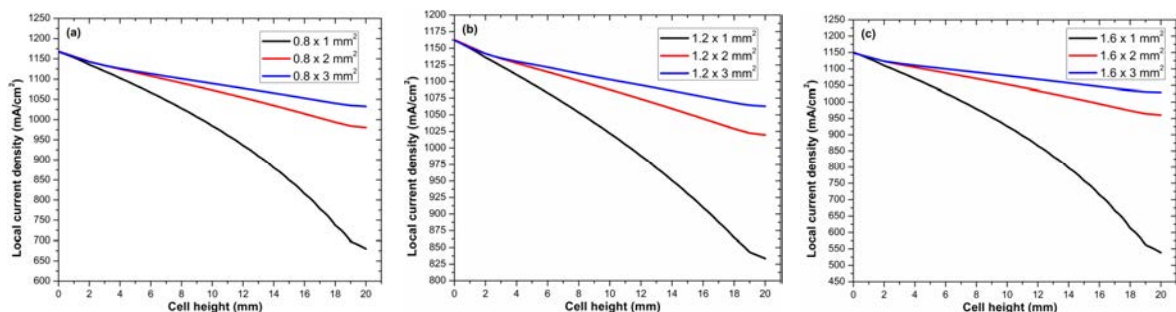


Fig. 4. Local current density variation along the cell height at a cell potential of 0.3 V and gas flow velocity of 0.1 m/s for various gas channel geometries: a) 0.8x1 mm<sup>2</sup>, 0.8x2 mm<sup>2</sup>, 0.8x3 mm<sup>2</sup>; b) 1.2x1 mm<sup>2</sup>, 1.2x2 mm<sup>2</sup>, 1.2x3 mm<sup>2</sup>; c) 1.6x1 mm<sup>2</sup>, 1.6x2 mm<sup>2</sup>, 1.6x3 mm<sup>2</sup>.

Fig. 5 showed the distribution of oxygen molar concentration in the cathode part of the cell model, for three channel geometries: 1.6x1 mm<sup>2</sup>, 1.6x2 mm<sup>2</sup> and 1.6x3 mm<sup>2</sup>. The point of interest in this figure is related to the concentration distribution in the cathode catalyst layer – GDL channel interface.

In Fig.5a we have seen that oxygen molar concentration in the gas channel and at the catalyst layer - GDL channel interface is nearly equal, whereas in fig.5.b and fig.5.c we observed that the molar concentration at the GDL – gas channel interface is much larger than in the catalyst layer. The cell performance is limited in all this cases for various reasons: in the case (a) channel presented a higher resistance to buoyancy flow and in the cases (b) and (c) porous media offered a significant diffusion resistance.

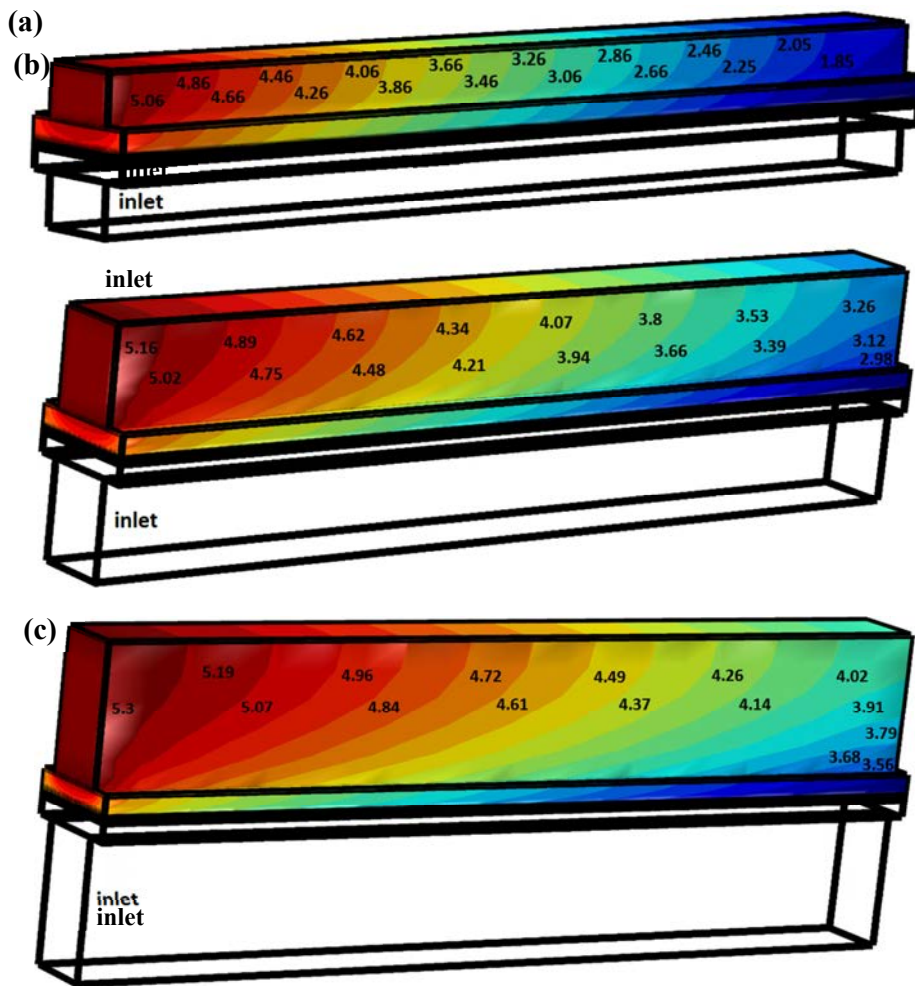


Fig. 5. Distribution of the oxygen molar concentration (mole/m<sup>3</sup>) along the cathode side of the cell for different gas channels geometries: (a)1.6x1 mm<sup>2</sup>, (b)1.6x2mm<sup>2</sup> and (c)1.6x3 mm<sup>2</sup>

Fig. 6 presented the variation of water and oxygen molar concentrations at cathode catalyst layer along the cell depth for three selected gas channel geometries: 0.8x3 mm<sup>2</sup>, 1.2x3 mm<sup>2</sup> and 1.6x3 mm<sup>2</sup>.

Water vapor is generated in the cathode catalyst layer due to electrochemical reactions and hence the water vapor molar concentration should increase along the cell depth. The most uniform distribution of oxygen molar concentration was registered for 1.6x3 mm<sup>2</sup> channel geometry (see fig. 6.a)

When the channel width was at the highest value of 1.6 mm, larger amount of air entered the cell and hence a lot less amount of dilution taken place due to water addition, as we could see from fig. 6.b.



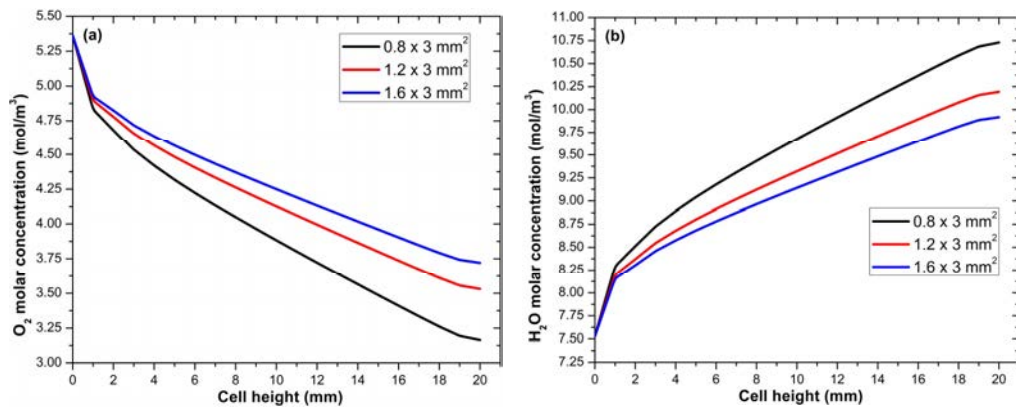


Fig.6. Variation of oxygen molar concentration (a) and water molar concentration (b) along the cell height for different gas channel geometries.

#### 4. Conclusions

In this paper, a steady-state 3D computational model was established to study the performance of a single HT-PEM fuel cell under varying gas channel parameters.

Preserving gas channel height constant and varying its width, current density registered a maximum value at one specific value of width for every gas flow velocity under study: 0.04 m/s, 0.06 m/s, 0.1 m/s, 0.12 m/s and 0.42 m/s. Instead, by maintaining width constant and modifying height, current density remained almost constant starting from one specific height value, also different for each of the gas flow velocity.

With a gas channel height of 1 mm, the performance of the cell is limited by the higher flow resistance offered by the channel, whereas for channel height of 2 mm and 3 mm the performance is limited due to a diffusion resistance offered by the porous media.

Local current density presented the most uniform variation along the fuel cell with  $0.8 \times 3 \text{ mm}^2$ ,  $1.2 \times 3 \text{ mm}^2$  and  $1.6 \times 3 \text{ mm}^2$  gas channel geometries due to more amount of oxygen entering the channel.

#### References

- [1] Segura F, Andujar JM, Duran E, Analog Current Control Techniques for Power Control in PEM Fuel-Cell Hybrid Systems: A Critical Review and a Practical Application, IEEE Trans. Ind. Electron. 2011; 58: 1171-1184.
- [2] Jia J, Wang G, Cham YT, Wang Y, Han M, Electrical Characteristic Study of a Hybrid PEMFC and Ultracapacitor System, IEEE Trans. Ind. Electron. 2010, 57: 1945-1953.
- [3] Nguyen TV, Water management by material design and engineering for PEM fuel cells, ECS Trans. 2006, 3: 1171-1180.
- [4] Abtahi H, Zilouchian A, Saengrungs A, Water Management of PEM fuel cells using fuzzy logic controller system, 2005 IEEE International Conference on Systems, Man and Cybernetics-SMC, Waikoloa, USA, 3486-3490, 10-12 October 2005.
- [5] Petrone G, Cammarata G, Modelling and Simulation, Croatia: InTeach Education and Publishing; 2008. p. 677-678.
- [6] Zhang J, Xie X, Tang Y, Song C, Navessin T, Shi Z, Song D, Wang H, Wilkinson DP, Liu ZS, Holdcroft S, High temperature PEM fuel cells, J. Power Sources 2006; 160: 872-891.
- [7] Berning T, Djilali N, A 3D, multiphase, multicomponent model of the cathode and anode of a PEM fuel cell, J. Electrochem. Soc. 2003; 150: 1589-1598.
- [8] Ubong EU, Shi Z, Wang X, Three-Dimensional Modeling and Experimental Study of a High Temperature PBI-Based PEM Fuel Cell, J. Electrochem. Soc. 2009; 156: 1276-1282.
- [9] Henriques T, César B, Costa Branco PJ, Increasing the efficiency of a portable PEM fuel cell by altering the cathode channel geometry: A numerical and experimental study, Applied Energy 2010; 87: 1400-1409.